

XII National and III International Conference on Engineering Thermodynamics

June 29th to July 1st 2022

Universidad Carlos III de Madrid: Campus de Madrid - Puerta de Toledo





XII National and III International Conference on Engineering Thermodynamics

Madrid, June 29th to July 1st, 2022

uc3m | Universidad **Carlos III** de Madrid

Proceedings Book

Edited by Antonio Acosta Iborra, Carolina Marugán Cruz and
Sergio Sánchez Delgado

ISBN: 978-84-09-42477-1

Contents

Organizing Committee	xi
Scientific Committee	xiii
Message from the Organizing Committee	xvii
I Full papers	xix
1 Energy efficiency and sustainability in buildings and industry	1
1.1 Comparative studies of different materials to store thermal energy for high-temperature applications	2
1.2 Kinetic study of biolubricant synthesis from fatty acid methyl esters through transesterification with pentaerythritol	10
1.3 The Heat Loss Coefficient decoupling method to obtain the Transmission and Infiltration heat loss coefficients of an in-use open office of a building	17
1.4 Energy rehabilitation of a construction quality control laboratory	25
1.5 Comparative life cycle assessment of energy-efficient buildings in Ireland’s rural area with current and future electricity mix scenarios	35
1.6 Techno-economic evaluation of different technologies to produce steam at 150°C in the Spanish industry	45
1.7 Energy study of new efficient thermal installations for a block of flats in Burgos (Spain) .	54
1.8 Machine Learning techniques for estimation of BIPV production	63
1.9 Indoor Daylight Model for All-Sky-Type Luminance Patterns	69
1.10 Analysis of low-cost sensors for solar illuminance measurement	79
1.11 Building’s thermal inertia detection using LSTM neural networks to improve the estimations of thermal demands	86
1.12 Energy model development of an office	95
1.13 Multi-objective optimization of the construction variables of a housing typology in the Metropolitan Region of Chile incorporating Pinus radiata wood impregnated with a phase change material	105
1.14 Numerical assessment of different low GWP alternatives for high temperature heat pumps using low temperature heat source	115
1.15 Analysis of stratification in a hot water production system using a CO2 transcritical heat pump	125
1.16 Physical measurements for the characterization of energy poverty	135
1.17 Integration of Combined Cooling, Heating and Power Microgrids to reach Zero-Energy Buildings	146

2	Energy, exergy and economic analysis and thermal power plants	155
2.1	Sizing and simulation of a solar thermal power plant that operates with a HRB cycle . . .	156
2.2	Thermodynamic analysis and optimization of an Organic Rankine Cycle driven by parabolic trough collectors	166
2.3	Tired of maximizing efficiency: the sCO ₂ recompression cycle might not be the best . . .	176
2.4	Preliminary integration of a two pressure-level solar steam generator in an ISCC with moderate and low temperature management	185
2.5	Study on the implementation of different thermal energy storage concepts in CSP plants .	195
2.6	Reference state temperature influence in the unit exergy consumption values	202
2.7	Exergetic and economic optimization of a novel thermal energy storage system based on granular material	212
2.8	Energy analysis for hydrogen transport methods	222
2.9	Development of Carbon/PPy/Pt Electrodes for Direct Methanol Fuel Cells	232
3	Experimental heat and mass transfer processes	239
3.1	Experimental study of a LiCl/Silica gel sorption thermal energy storage prototype	240
3.2	Convection heat transfer coefficient study in a bayonet heat exchanger	249
3.3	Thermal performance of an additively manufactured heat pipe with grooved wick	259
3.4	Compact climatization system for mechanical ventilation with heat recovery	266
3.5	Hydrogen and carbon utilization through Power to Gas. Experimental activities for carbon recycling and renewable H ₂ injection into the grid	274
3.6	Experimental characterization of solar central receivers	284
3.7	Improvement of heat dissipation in a thermal conductivity test bench	294
3.8	Comparative study on bubbling and shearing techniques for the crystallization of xylitol in TES systems	304
4	Fuels, combustion, pyrolysis and gasification	315
4.1	Autoignition of a diesel/OME3-5 blend under dual-fuel combustion with methane	316
4.2	Combustion diagnosis on a dual CI engine fueled with methanol	324
4.3	Optimization of the operating conditions of a biomass boiler fueled with almond shells . .	334
4.4	Thermal study of a liquid metal solar reactor for methane pyrolysis	340
4.5	An experimental study on poultry industry-derived solid biofuels	349
4.6	Experimental study of biomass combustion emissions	359
4.7	Bibliometric study on dual-fuel injection	367
4.8	Experimental Evaluation of Methane-Hydrogen Fuel Blends for Stable Lean Operation in Spark Ignition Engines	377
4.9	Recovery of fibre, oil and gas by controlled pyrolysis of end of life composites from wind turbine blades	387
5	Thermal engines, heat exchangers and their subsystems	399
5.1	Axial-flow turbines operating at part load under similarity conditions with different gases	400
5.2	Development of an experimental test rig for the characterization of aerothermal effects derived from the miniaturization of radial turbocompressors	407
5.3	Autonomous thermoelectric generators for volcanic surveillance	415
5.4	Experimental analysis of flexible thermoelectrics for energy harvesting	425
5.5	Thermal design of once-through coil-wound steam generator for solar power plants	433
5.6	Analysis of frost formation in an air-to-water heat pumps' Coil Heat Exchangers	444
5.7	Asymptotic analysis of superadiabatic small-scale combustors with a two-step chain-branching chemistry model	454

6	Numerical simulation and modelling	461
6.1	Numerical Investigation of a Trapezoidal Cavity Multi-tube Receiver for a Linear Fresnel Collector	462
6.2	Radiative collectors and emitters to improve the efficiency of compression heat pumps . .	472
6.3	Flow and heat transfer of a gas-particle dense suspension in a tube for CSP applications: numerical analysis	482
6.4	Modeling sensible thermal energy storage in solid blocks for concentrating solar power . .	492
6.5	Detailed numerical simulation of corrugated receiver tubes for molten salt solar power towers	502
6.6	Analysis of the thermal inertia of pipelines in SHIP	512
6.7	Numerical model of water/lithium bromide falling film absorbers	522
6.8	Analysis of the cooling capacity of a transformer at low ambient temperatures with different dielectric fluids: mineral oils and esters, using CFD	532
6.9	Regional modeling of the potential of rooftop photovoltaics for the Tarragona province . .	542
6.10	An extended Benson-based group contribution method for the estimation of the heating value of terpenic biofuels	552
6.11	Comprehensive analysis of hot water tank sizing for a hybrid solar-biomass district heating and cooling	559
6.12	Analysis of the absorptance and emittance in particle receivers by means of a discrete MCRT method	569
6.13	Numerical Simulation of Convective Heat Transfer Coefficient in Wire Mesh Absorbers with fixed porosity	579
6.14	Deep learning optimal control for a solar-biomass system for residential buildings	589
6.15	Numerical simulation of a fluidized bed with an immersed tube bundle heat exchanger . .	598
6.16	A 1D numerical model for a high temperature, shell-side enhanced latent thermal energy store	607
6.17	Pressure drop effect on recompression CO2 Brayton cycle	615
6.18	Applicability of high reflective roof coatings on the Spanish existing building stock over different climate zones	625
6.19	Numerical study of isothermal flow in an active LHES system based on a SSHE	635
6.20	Numerical model of a Cooling system for a MgB2 based HVDC Superconducting Link. Assessment and behavior of coolants	646
6.21	Comparison of spatial interpolation methods for the estimation of solar potential in Castilla y León	655
6.22	Experimental and numerical simulation study of a PCM melting process without convective flows	661
6.23	Packaging configuration analysis for a lithium-ion battery module	670
6.24	Integrated thermal management in hybrid vehicles by means of numerical simulation . . .	680
6.25	Combustion modeling in a pressurized gas turbine burner using Large-Eddy Simulations .	690
6.26	Design and Optimization of Composite Cylindrical Spines Using the Relative Inverse Thermal Admittance under Convection and Radiation Conditions	700
6.27	Numerical comparison of an ultrasonic mist generator and an ultrasonic spray atomizer used as evaporative coolers	710
6.28	Analysis of operating conditions of water/air cooled water/LiBr absorption chillers for cooling and heating applications	720
6.29	Numerical evaluation of the impact of a mechanical attachment on the preheating of an external tubular receiver	730
6.30	Suppression of thermoacoustic instabilities by flame-structure interaction	740
6.31	Thermodynamic simulations of the effect of pressure on high-temperature corrosion under a supercritical CO2 environment	744
6.32	The wavemaker of puffing pool fires	751
6.33	Forced fluid flow in a solar wood-dryer: numerical study	758

7	Refrigeration, thermal comfort and air conditioning	765
7.1	Spatiotemporal estimations of thermal comfort conditions inside existing buildings using MLP neural networks	766
7.2	Use of NSGA-III combined with MLP neural networks for optimising spatiotemporal estimations of thermal comfort in buildings	776
7.3	Thermo-hydrodynamic constraints of the thermal compressor on the performance of an NH ₃ /H ₂ O absorption chiller	786
7.4	Determination of dead state in exergy analysis of absorption chillers	796
7.5	Sensitivity analysis of the geometrical parameters in cyclone oil separators for ultra-low charge ammonia chillers	806
7.6	Thermo-economic evaluation of different condensing strategies in ultra-low charge ammonia chiller	815
7.7	Experimental start-up of ultra-low temperature unit retrofitted with R170	823
7.8	Genetic algorithm validation to simulate refrigerant mixtures in ultra-low temperature equipment	829
7.9	Experimental Energy evaluation of the Internal Heat Exchanger mounted in a horizontal freezing cabinet using R404A and its low-GWP alternatives	835
7.10	Low-GWP hydrocarbons blends as an alternative for the HFC R134a. Energy assessment in a vertical beverage cooler	847
7.11	Cooling water systems for industrial plants	856
7.12	Design and operation considerations of the pipe systems of wet cooling towers in power plants	866
8	Renewable energies, environmental impact and circularity	877
8.1	Hydrogen from municipal solid waste as a tool to compensate unavoidable GHG emissions	878
8.2	Hybrid Brayton supercritical CO ₂ power cycle using a gas turbine and a tower solar receptor with an ORC as a waste heat recovery system	887
8.3	Trends and Gaps on the Research of Integration of Solar Photovoltaic Power Plants into Power Networks through a Bibliometric Analysis	897
8.4	Life Cycle Assessment (LCA) of alternative mortars to Portland cement: carbon and water footprint according to unit of stored energy	907
8.5	Experimental development of a thermoelectric generator without moving parts to harness hot dry rock fields	917
8.6	Analysis and optimization of solar thermal systems for buildings	926
8.7	Computational study of geothermal thermoelectric generators with phase change heat exchangers	937
8.8	ASTEP Concept: Design and Simulation of a Solar Heating System for a Dairy Industry .	945
8.9	Estimation of the solar thermal power generation potential in Pamplona (northern Spain)	955
8.10	Air thermal behavior in Madrid Calle 30 tunnels	965
8.11	Air as a residual energy collector system in Metro de Madrid tunnels	973
8.12	Extension of Locally Adapted Models of Photosynthetically Active Radiation for All Sky Conditions	981
8.13	Spectral Distribution of Solar Radiation under CIE Standard Sky Condition	987
8.14	Optimization of solid fuel briquettes from waste biomass from Luanda -Kwanza Sul - Huambo corridor, Angola	994
8.15	Modeling of Beam-down linear Fresnel conveyor dryer for bulk solid processing	1004
8.16	Assessment of by-products materials for concentrated solar power plants (CSP): Physico-chemical, morphological, thermal and solar absorption study	1014
8.17	Calculation of intercepted photosynthetically active radiation (IPAR) for traditional crops in Castilla y León, Spain	1024
8.18	Technical viability of different Power to Gas integration configurations in a BF-BOF iron and steel plant	1032

8.19	CSP plants performing a Brayton cycle: a comparative analysis of central tower and parabolic dish farms	1042
8.20	Real-time measurement of solar irradiance with field hyperspectral spectroradiometer and comparison with modelling	1052
8.21	Waste tyre pyrolysis gas cleaning from hydrogen sulfide	1065
8.22	A Unit-cell Model of Vanadium Redox Flow Batteries: The Role of Operating Conditions	1071
8.23	Phenanthrene accessibility to the active sites in USY zeolite-based platinum catalyst: The effect on phenanthrene hydrocracking reaction	1078
8.24	Detailed analysis of sulfur contaminants derived from air-blown fluidized bed gasification of waste tires	1088
8.25	CCS, know-how and foreseen challenges of the capture and compression stages from a Process engineering point of view	1096
8.26	Concentrating Solar Thermal Technologies – Status, Cost and Research Trend	1103
9	Teaching innovation and digital education tools	1113
9.1	Development of virtual lab practices of industrial refrigeration using the Engineering Equation Solver to facilitate remote access to students	1114
9.2	User’s role in building performance simulation: Experiments conducted at practice sessions in an engineering master’s degree	1121
9.3	New teaching methodologies: learning through applied research in experimental convective heat transfer for undergraduate students	1129
9.4	ALMIA Educativa as an educational strategy towards an effective energy transition of a rural village	1136
9.5	Transition to online teaching in Thermal Engineering during the pandemic situation	1141
10	Thermodynamics and climate change	1151
10.1	Experimental Study of a Multistage Thermoelectric Heat Pump for Thermal Energy Storage	1152
11	Thermo-physical properties of materials and fluids	1159
11.1	Viscosity as a suitable parameter to monitor biolubricant production from vegetable oils	1160
11.2	Nanofluid preparation and experimentation in a flat plate solar thermal collector	1166
11.3	LLE of binary mixtures 3-phenyl-1-propanol+alkanes	1176
11.4	Thermophysical property needs for decarbonising the gas grid	1184
11.5	Measuring trace water in ultra-high purity gases	1190
11.6	Vapor pressure measurements and Near-Infrared analysis of binary and ternary solutions with H ₂ O, LiBr and [Dmim][Cl]	1195
11.7	Combustion Toolbox: an open source thermochemical code for solving gaseous combustion problems	1201
11.8	Characterization of a Lambertian target	1211
II	Poster abstracts	1221
1	Energy efficiency and sustainability in buildings and industry	1223
1.1	Comparison of strategies to control a movable wall with PCM	1224
1.2	ASTEP: Application of Solar Thermal Energy to Processes. Current status and progress	1226
1.3	Effect of phase change materials on the properties of lime mortars	1228
1.4	Solar District Heating and Cooling Network in Spain	1230
2	Energy, exergy and economic analysis and thermal power plants	1233
2.1	Brayton supercritical CO ₂ cycles as pumped thermal energy storage (PTES) for industry applications	1234

2.2	AdInCCSol: Advanced Integration of Combined Cycles in Solar Thermal Power Plants. Current status and progress	1236
2.3	CTR design methodology proposed for the project AdInCCSol	1238
2.4	Performance analysis of supercritical carbon dioxide recompression cycles under different ambient temperature conditions, integrating mean line turbomachines models	1240
2.5	Preliminary exergy analysis of ASTEP system	1242
3	Experimental heat and mass transfer processes	1245
3.1	Crystallization on polyols. Intercomparison between xylitol, erythritol and its eutectic mixture	1246
3.2	Aging MgCl ₂ /Mg(NO ₃) ₂ /H ₂ O mixture improvement for latent heat storage	1248
4	Fuels, combustion, pyrolysis and gasification	1251
4.1	Automatic classification of biomass PM emissions by means of Machine Learning techniques	1252
4.2	Activated carbon for the capture of Volatile Organic Compounds from biomass combustion. A study on aging and conservation of the samples	1254
4.3	3-stage combustion analysis of a heavy-duty diesel engine fueled with binary blend	1256
4.4	Comparative study of woody and non-woody biomasses in a small-scale combustion system with air stratification and FGR	1258
4.5	Experimental study of an autothermal portable reformer	1260
4.6	Elucidating pathways for the formation of secondary hydrochar from biomass HTC	1262
4.7	Renewable synthetic hydrocarbons from CO ₂ or CO through the use of bifunctional catalysts	1265
4.8	Can the ashes of a char be tuned up by HTC?	1269
4.9	Repeatability of PM charge measurements with biomass combustion	1272
6	Numerical simulation and modelling	1275
6.1	Simulation of bed dynamics inside a gasifier with rotary mechanisms	1276
6.2	CFD study of flame confinement in a small-scale biomass combustion system using porous inert material	1278
6.3	A machine learning approach for parametric study on enhanced surfaces characterization	1280
6.4	Computational study of CO ₂ concentration inside a classroom with different air condition- ing distributions	1282
7	Refrigeration, thermal comfort and air conditioning	1285
7.1	Modelization of an elastocaloric cooling cycle	1286
8	Renewable energies, environmental impact and circularity	1289
8.1	Preliminary design of two SunDial collectors for Solar Heat for Industrial Processes at different latitudes	1290
8.2	Transcritical power cycles for pumped thermal energy storage systems	1292
8.3	Proposal and simulation of a multi-tube receiver for Fresnel collector	1294
8.4	Environmental and economic impact of personal electric urban mobility	1296
8.5	Carbon recycling in ironmaking through power to gas and oxygen blast furnaces	1298
8.6	"In-situ" and "ex-situ" characterization methods for PEM-type fuel cells. Application to the BALLARD 1.2 kW stack	1300
8.7	Valorisation of spent coffee grounds in energy recovery processes: evaluation of thermal and thermo-oxidative decomposition	1303
8.8	Inorganic filler to improve dielectric and proton conductivity of fuel cell membranes . . .	1305
9	Teaching innovation and digital education tools	1307
9.1	Blended Learning Experience using Virtual Water Level Control Lab	1308
9.2	Improving the long-term learning in Engineering Thermodynamics through spaced review to overcome Ebbinghaus' forgetting curve	1310

11 Thermo-physical properties of materials and fluids	1313
11.1 Understanding the thermo-physical properties of nanofluids	1314
11.2 Thermophysical Study of Binary Mixtures of Organic Compounds as Potential Base Material for Nano Enhanced Phase Change Materials	1316
11.3 An experimental investigation on thermal conductivity of aqueous theta-phase aluminum oxide nanofluids	1318
Authors Index	1321



Energy analysis for hydrogen transport methods

Vladimir L. Meca¹, Rafael d'Amore-Domenech¹, Antonio Villalba-Herreros¹, Teresa J. Leo¹

¹Affiliations: Dept. Arquitectura, Construcción y Sistemas Oceánicos y Navales, ETSI Navales, Universidad Politécnica de Madrid, Avenida de la Memoria 4, Madrid 28040, Spain, vl.meca@upm.es

Keywords: Maritime transport; hydrogen; methanol; energy vector; alternative fuels; seaborne.

TOPIC: Energy, exergy and economic analysis and thermal power plants

1. Abstract

A comparative energetic study between liquid hydrogen and e-methanol as hydrogen vectors for large-scale transport of hydrogen at sea has been performed. The objective of this study is to gain insight on which one of the energy vectors compared is the best option for transporting renewable energy and obtain hydrogen at destination. The alternatives covered include the seaborne transport of liquid hydrogen or methanol with the reconversion to hydrogen at the destination through methanol electrolysis or a steam-reforming process. Three different production mass flow rates of hydrogen at the origin are explored: 100 kt/y, 1 Mt/y, and 10 Mt/y. The findings of this study suggest that liquid hydrogen is the best alternative in terms of energy vector. However, if methanol electrolysis technology improves, lower electricity consumption and lower energy losses are achieved, the alternative based on methanol electrolysis may compete with the transport of liquefied hydrogen.

2. Introduction

There is an increasing importance of renewable energies in the global power sector. However, the renewable energy sources may not be close to the place of energy consumption, which makes it necessary to transport this energy to its destination. In addition, some of them, such as wind and solar energy, have stochastic and intermittent nature due to their dependence on weather conditions. A possible solution consists of the storage and transport of this energy to adapt its consumption to the needs of existing energy grids. Renewable electrical energy could be stored in the form of chemical energy of a fuel, such as green hydrogen [1].

Green hydrogen can be generated through water electrolysis with electricity from renewable sources and then transported to the destination [2]. However, due to the low energy density of hydrogen (the energy per volume of hydrogen gas is 12.7 MJ/Nm³, merely 1/3000 of oil) the seaborne transport of this fuel is carried out in tankers that transport liquefied hydrogen (LH₂). Regarding the safety, LH₂ induces hydrogen embrittlement and well-designed vessel and containment facilities must be designed to contain this fuel. Besides, a small release or leakage of LH₂ potentially results in explosion.

A fuel that can be obtained from green hydrogen and that is easier to handle than a gaseous fuel is methanol (MeOH), as it is a liquid chemical compound at ambient conditions. Methanol has lower impact than conventional hydrocarbon fuels if leaked into the environment due to the fact that it dissolves readily in water. Furthermore the International Bulk Chemical Code does not classify it as a toxic substance if it is onboard cargo. Once at destination, this methanol can be used as fuel or converted into hydrogen. In this way, one of the applications of methanol as an energy vector arises, being an energy transport option that could constitute a way of transporting clean energy from its origin to its place of consumption. The methanol obtained through

captured CO₂ and hydrogen from renewable sources, e-methanol, is neutral in carbon emissions. For the conversion of e-methanol into hydrogen there are different possibilities, among which steam reforming and electrolysis stand out [3].

In this work the energy analysis of three alternatives for seaborne transport of hydrogen is presented. The first one is based on LH₂ transport and the other two options are based on MeOH transport.

The alternative based on the transport of liquefied hydrogen includes water electrolysis plant, hydrogen liquefaction plant, storage at origin, transport, storage at destination and hydrogen regasification plant.

Alternatives based on the transportation of methanol include water electrolysis plant, methanol synthesis plant, storage at origin, transportation and storage at destination. The difference within methanol-based alternatives is established in the process to obtain hydrogen at destination. In one of them the electrolysis of methanol is carried out and in the other the methanol steam reforming is studied.

Three different mass flow rates of hydrogen produced are studied: 100 kt/y, 1 Mt/y and 10 Mt/y. The distance analysed corresponds to seaborne transport between Brazil and Spain. Brazil is one of the main methanol producers, and its low electricity cost makes green hydrogen production attractive. Spain has been selected as green fuel importer as there is an increasing demand for carbon-neutral fuels in Europe, and Spain can be an important hydrogen distribution point in the Mediterranean Sea.

3. Methods

In this study, an energetic analysis of the sea transport of energy from renewable sources using hydrogen and e-methanol as vectors is made. The route proposed is Pecem (Brazil) - Algeciras (Spain), a distance of 5629 km.

Hydrogen is obtained from water with an electrolysis process consuming electricity from renewable sources, and this hydrogen is liquefied and transported as liquefied hydrogen or transformed into e-methanol through a synthesis process for transporting e-methanol by ship.

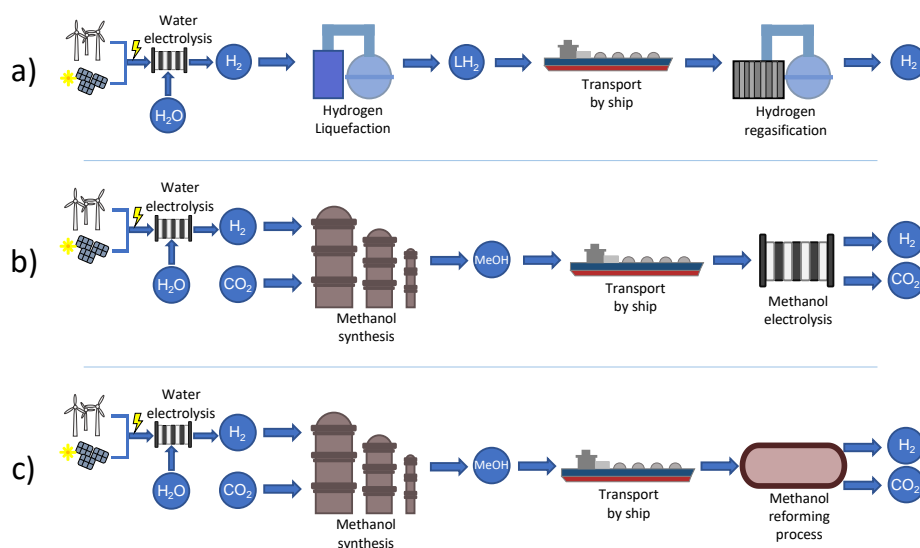


Figure 1. Diagram of the hydrogen transport process using as a vector: a) liquefied hydrogen (LH₂); b) methanol (MeOH) with electrolysis process; c) methanol (MeOH) with reforming process.

In this study, three alternatives are analysed, presented in Figure 1: one based on the transport of liquefied hydrogen (Figure 1.a) and two on the transport of e-methanol. The alternatives based on the transport of e-methanol differ from each other when obtaining hydrogen at destination, from an electrolysis process (Figure 1.b) or a reforming process (Figure 1.c). To carry out this study, the mass flow of hydrogen available at the place of origin is established (100 kt/y, 1 Mt/y and 10 Mt/y). The three alternatives proposed in this work are presented in Subsections “3.1. Hydrogen power link”, “3.2. Methanol power link with electrolysis process” and “3.3. Methanol power link with reforming process”.

The initial energy flow of the analysis of this work is the electricity supplied to the electrolyser to obtain hydrogen from water, that is part of the hydrogen production process of each alternative. Its characteristics are presented below.

Water electrolysis plant. In this facility, hydrogen and oxygen are produced using renewable electricity and water. To develop this model, the efficiency of the water electrolyser has been set at 80 % [4]. From this parameter and the desired hydrogen mass flow rate, the mass flow rates of necessary water, $\dot{m}_{\text{H}_2\text{O}}$, and oxygen produced, \dot{m}_{O_2} , during the process and the electric power consumed, $\dot{W}_{\text{ext,electrol}}$, have been calculated using Eq. 1 and 2, respectively.



$$\dot{W}_{\text{ext,electrol}} = \frac{\dot{m}_{\text{H}_2} \cdot h_{\text{H}_2} + \dot{m}_{\text{O}_2} \cdot h_{\text{O}_2} - \dot{m}_{\text{H}_2\text{O}} \cdot h_{\text{H}_2\text{O}}}{\eta_{\text{electrol}}} \quad (\text{Eq. 2})$$

where $\dot{m}_{\text{H}_2} = M_{\text{H}_2}/M_{\text{H}_2\text{O}} \cdot \dot{m}_{\text{H}_2\text{O}}$; $\dot{m}_{\text{O}_2} = M_{\text{O}_2}/M_{\text{H}_2\text{O}} \cdot \dot{m}_{\text{H}_2\text{O}}/2$, and h_i is the the enthalpy of the different substances present in the reaction that is calculated as:

$$h_i = \Delta h_{f_i}^0 + [h_i(T, p) - h_i(T^0, p^0)] \quad (\text{Eq. 3})$$

where $\Delta h_{f_i}^0(T^0, p^0)$ is the enthalpy of formation of the substance i at (T^0, p^0) , and $[h_i(T, p) - h_i(T^0, p^0)]$ is the enthalpy increment of the substance i from (T^0, p^0) to (T, p) .

3.1. Hydrogen power link

Hydrogen can be transported by sea under different conditions, such as liquefied and compressed hydrogen by ship. Due to the low energy density of the on-board compressed hydrogen storage system compared to liquefied hydrogen, the last option is chosen for comparison purposes with the methanol vector within this study. Figure 1.a shows a diagram of this alternative.

The characteristic facilities of this alternative are:

Hydrogen liquefaction plant. This facility liquefies the hydrogen obtained from electrolysis to transport it more easily. The electrical energy needed for the transformation of hydrogen into a liquefied state is calculated by multiplying the mass of the produced hydrogen by the specific work for hydrogen liquefaction (22.0 MJ/kg)[5].

Liquid hydrogen storage facilities. The storage of liquid hydrogen after and prior to its transport is an important facility within the power link. The size of the tanks of the export terminal is adapted to that of the tanks of the ship that will transport the liquefied hydrogen. The size of the installation prepared for import is dependent upon the number of ships, voyages, and mass of hydrogen that they deliver. The electricity consumption within this installation is related to re-liquefaction energy of the boil-off of the stored hydrogen. A daily boil-off rate of 0.1 % of the total mass of hydrogen contained in the tanks is considered [2]. The energy needed for the re-liquefaction process is calculated with the specific work for hydrogen liquefaction.

LH₂ carrier ship. Currently there is no fleet of hydrogen transport vessels, but there are vessels that can undertake this operation [6]. Nevertheless, there is insufficient data regarding these types of ships in order to create a model and it has been decided, due to the similarities they present, to use data from LNG transport fleets, thereby adapting them for purposes of creating a transport model of liquefied hydrogen. Regarding fuel consumption, in this work, ships that transport hydrogen as cargo are assumed to consume part of the hydrogen cargo for propulsion with a power plant based on fuel cells. Therefore, the consumed cargo during the round trip will be considered in the energy analysis. The consumed mass of hydrogen m_C is estimated by means of:

$$m_C = 2 \cdot \frac{l}{s_V} \cdot cr_C + \left(\frac{V_H}{\dot{V}_L} + \frac{m_{OL}}{\rho_l^0 \cdot \dot{V}_{OL}} \right) \cdot cr_{L,OL} \quad (\text{Eq. 4})$$

where l is the distance between ends, s_V is the speed of the vessel, cr_C is the consumption rate of hydrogen during navigation, V_H represents the volume of the holds inside the ship, \dot{V}_L is the loading flow rate of the liquefied hydrogen, m_{OL} is the offloaded mass of hydrogen, ρ_l^0 represents the saturation density of liquid hydrogen at 1 bar, \dot{V}_{OL} represents the off-loading flow rate of the liquefied hydrogen and $cr_{L,OL}$ is the consumption rate of hydrogen during loading and offloading.

The mass flow rate of hydrogen consumed during cruising, cr_C , can be calculated according to the cubic rule [2]:

$$cr_C = \frac{\dot{W}_{nom}}{\eta_{FC} \cdot LHV} \cdot \left(\frac{s_V}{s_{V_{nom}}} \right)^3 \quad (\text{Eq. 5})$$

where \dot{W}_{nom} is the power developed at cruise speed; η_{FC} is the fuel cell efficiency; LHV is the Lower Heating Value of hydrogen and $s_{V_{nom}}$ the nominal cruise speed of the ship.

Table 1 contains the baseline assumptions used for the calculations of the energy consumed within hydrogen power link.

Table 1. Assumptions for the LH₂ transport facility.

Parameter	Value
Ship capacity (t _{H2})	12,760
V_H (m ³)	180,000
Nominal pressure (bar)	1
Min pressure (bar)	1
$s_{V_{nom}}$ (kn)	20
$s_{V_{nom}}$ (m/s)	10.29
\dot{W}_{nom} (sailing) (MW) [7, 8]	35
\dot{W}_{nom} (Loading and offloading) (MW)	2
Power plant efficiency η_{FC} (based on LHV _{H2})	0.55
\dot{V}_L (m ³ /h)	12,000
\dot{V}_{OL} (m ³ /h)	12,000

Hydrogen regasification. Some facilities of this type use heat exchangers to obtain hydrogen under conditions suitable for storage in vehicles. The thermal energy required to evaporate the liquefied hydrogen in those heat exchangers is calculated from the enthalpy difference of the liquefied hydrogen and hydrogen at standard conditions of pressure and temperature.

3.2. Methanol power link with electrolysis process

This power link raises the possibility of using e-methanol as a hydrogen vector. It is based on the transport of this fuel obtained using green hydrogen and CO₂ as feedstocks, and subsequently, obtaining hydrogen at destination by carrying out a methanol electrolysis process. Figure 1.b shows a diagram of this alternative.

The characteristic facilities of this alternative are:

Methanol synthesis plant. Within this facility methanol is obtained through a synthesis process from renewable hydrogen and CO₂. The ratio between hydrogen and methanol mass flow rates and CO₂ and methanol mass flow rates needed in this facility are fixed (1.397 kg_{CO2}/kg_{MeOH}, 0.192 kg_{H2}/kg_{MeOH}) [9]. Electricity needed within this facility is also related to the mass flow rate of methanol produced, 0.175 MWh/t (630 kJ/kg) [9].

Methanol carrier ship. There are ships designed to transport methanol nowadays, however, not enough data have been collected to develop a reliable model. For this reason, the model developed for hydrogen transport has been used, adapting the input data to that of a tanker ship due to the similarities between ships presently transporting methanol and this type of ships. As in the case of hydrogen transport, methanol is intended to be used as fuel for propulsion, in this case in an internal combustion engine. Table 2 contains the baseline assumptions used for the calculations of the energy consumed within methanol power link.

Table 2. Assumptions for the methanol transport facility.

Parameter	Value
Ship capacity (t _{MeOH})	95,040
V _{MeOH} (m ³)	120,000
s _{V_{nom}} (kn)	15.4
s _{V_{nom}} (m/s)	7.92
Ẇ _{nom} (sailing) (MW)	15
Ẇ _{nom} (Loading and offloading) (MW)	2
Power plant efficiency η _{FC} (based on LHV _{H2})	0.35

Methanol electrolysis plant. In this facility hydrogen is obtained using renewable electricity and e-methanol. The model developed in this work is based on the efficiency of a methanol electrolyser, set at 34 % [10]. The mass flow rate of hydrogen obtained at the destination and the electric power needed for this process, Ẇ_{ext,MeOH electrol}, are calculated using Eqs. 6 and 7, respectively:



$$\begin{aligned} \dot{W}_{ext,MeOH\ electrol} \\ = \frac{\dot{m}_{\text{H}_2} \cdot h_{\text{H}_2} + \dot{m}_{\text{CO}_2} \cdot h_{\text{CO}_2} - \dot{m}_{\text{H}_2\text{O}} \cdot h_{\text{H}_2\text{O}} - \dot{m}_{\text{CH}_3\text{OH}} \cdot h_{\text{CH}_3\text{OH}}}{\eta_{meth-electrol}} \end{aligned} \quad (\text{Eq. 7})$$

where $\dot{m}_{\text{H}_2} = \frac{M_{\text{H}_2}}{M_{\text{H}_2\text{O}}} \cdot \dot{m}_{\text{H}_2\text{O}} \cdot 3$; $\dot{m}_{\text{CO}_2} = M_{\text{CO}_2}/M_{\text{H}_2\text{O}} \cdot \dot{m}_{\text{H}_2\text{O}}$; $\dot{m}_{\text{CH}_3\text{OH}} = M_{\text{CH}_3\text{OH}}/M_{\text{H}_2\text{O}} \cdot \dot{m}_{\text{H}_2\text{O}}$; and the enthalpies are obtained with Eq. 3.

3.3. Methanol power link with reforming process

This power link shares the characteristics of the case 3.2 previously described. The difference lies in the method for hydrogen production from methanol. In this case, hydrogen is obtained by means of a methanol-reforming process. The characteristics of the processes of this power link are the same as in the previous case, thereby exchanging the methanol electrolysis plant for a methanol-reforming one. Figure 1.c shows a diagram of this alternative.

Methanol-reforming plant. During this process, an input of thermal energy is needed to obtain hydrogen from e-methanol. To provide this thermal energy a portion of the transported e-methanol is burned. Due to this, the emission from the e-methanol combustion is added to the CO₂ emission produced during the reforming process, which is more difficult to capture than the CO₂ produced from electrolysis. However, this way of obtaining the necessary thermal energy makes the process independent from the electrical grid. The mass flow rate of methanol necessary to carry out the reforming process is obtained from the data of the efficiency of a methanol reforming reactor:

$$\dot{m}_{MeOH_{Combustion}} = \dot{m}_{MeOH} \left(1 - \frac{\frac{LHV_{MeOH}}{LHV_{H_2}} \cdot \eta_{reform}}{r_{conv}} \right) \quad (\text{Eq. 8})$$

where \dot{m}_{MeOH} represents the mass flow rate of methanol that arrives at the facility in kg/s, LHV represents the lower heating value of methanol and hydrogen in MJ/kg, η_{reform} represents the efficiency of the methanol reforming reactor, set at 85 %, and r_{conv} represents the mass ratio of hydrogen converted to methanol in the reforming process (0.189 kg_{H2}/kg_{MeOH}) [11].

4. Results

Figures 2-4 show the process energy flow diagram for an annual produced hydrogen of 100 kt, 1 Mt and 10 Mt, respectively. From left to right: hydrogen power link, methanol transport and electrolysis alternative, methanol transport and reforming alternative. To develop these diagrams, the value of 100 is assigned to the electricity from renewable sources necessary to conduct the water electrolysis in each case. The energy contained in the e-methanol and hydrogen vectors has been obtained with the LHV of each fuel.

Figure 2 shows the processes that require a higher electricity consumption, without considering the production of hydrogen from water: methanol electrolysis and hydrogen liquefaction. The processes that involve the greatest energy losses are the methanol electrolysis process, the synthesis of this fuel and the reforming of methanol to obtain hydrogen.

Figure 3 shows that for a mass flow rate of 1 Mt/y the methanol electrolysis alternative can provide better results in terms of hydrogen mass flow rate obtained at destination. However, the electricity consumption for the electrolysis process is greater than the electricity needed for hydrogen liquefaction. Thus, despite obtaining a slightly greater mass flow of hydrogen with methanol electrolysis alternative, hydrogen liquefaction still remains the best option in terms of energy.

Figure 4 shows the increase in methanol consumption with respect to the total electrical energy supplied at the source when the mass flow rate of hydrogen produced increases to 10 Mt/y. However, this figure also shows a decrease in the percentage of energy supplied for the methanol electrolysis and also in the energy losses of the processes for transforming hydrogen into methanol.

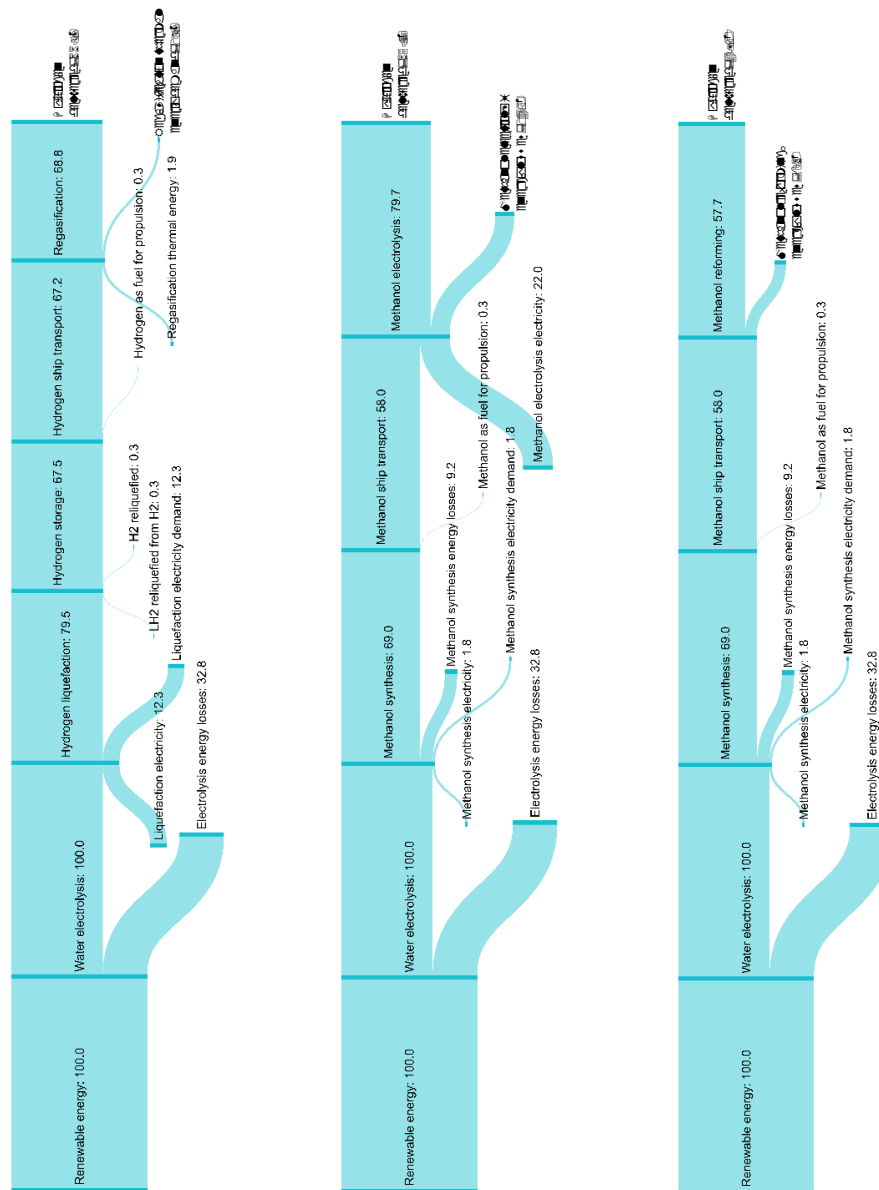


Figure 2. Process energy flow diagram for an annual production of 100 kt of hydrogen. From left to right: hydrogen power link, methanol transport and electrolysis alternative, methanol transport and reforming alternative. 17,870 TJ/y is set at an index value of 100.

In in Figures 2-4, the energy that reaches its destination in the form of hydrogen presents similar values between the alternatives based on liquefied hydrogen and on methanol electrolysis, with a maximum variation of 1.2 %. The energy that reaches the destination for the alternative based on steam reforming is 16.6 % lower than the obtained with methanol electrolysis alternative. This difference is due to the consumption of methanol to obtain the necessary thermal energy during reforming. Thus, to compare methanol electrolysis and methanol reforming alternatives, the electricity consumption of the methanol electrolysis must be considered.

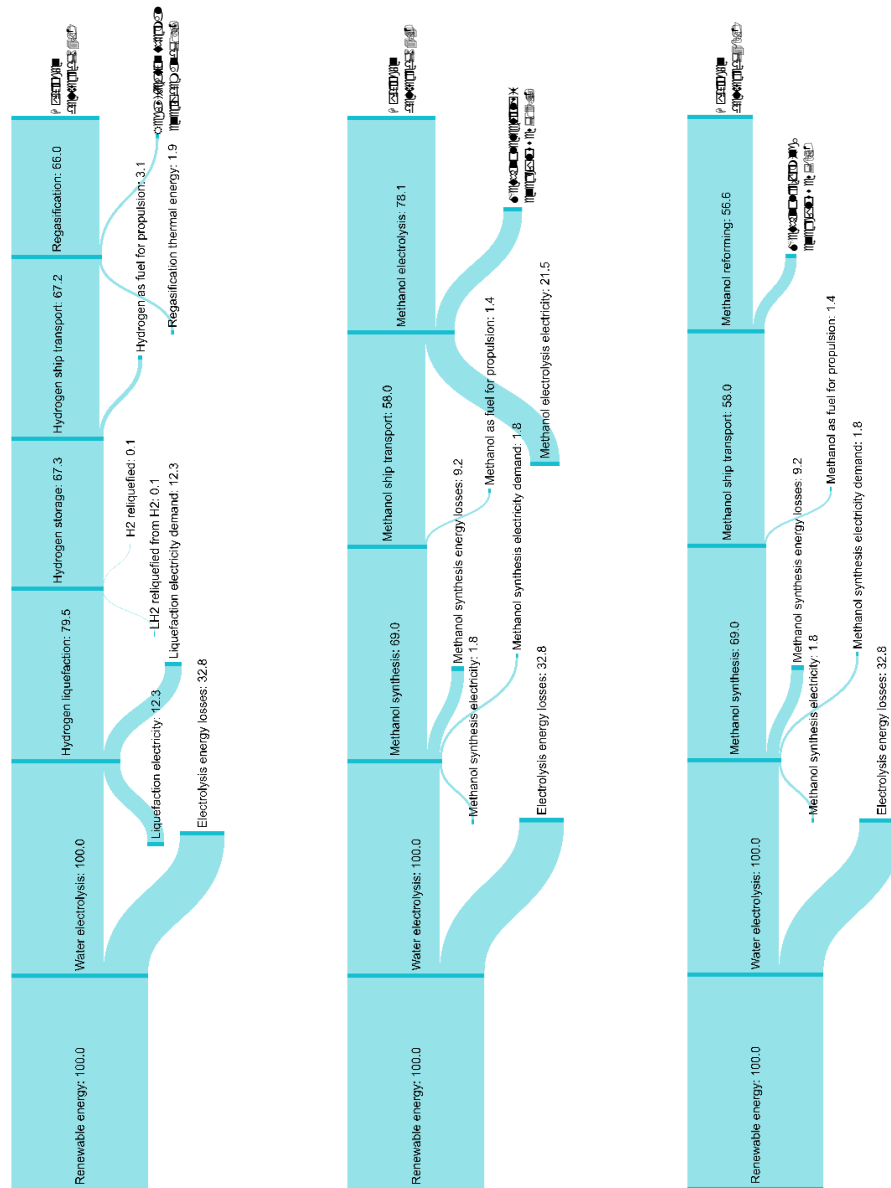


Figure 3. Process energy flow diagram for an annual production of 1 Mt of hydrogen. From left to right: hydrogen power link, methanol transport and electrolysis alternative, methanol transport and reforming alternative. 178,700 TJ/y is set at an index value of 100.

Figures 2-4 show that by increasing the hydrogen mass flow rate, the consumption of methanol and hydrogen for propulsion of the ships increases in relation to the electricity supplied for the electrolysis of the water in each power link. Besides, hydrogen consumption for propulsion represents a higher percentage of the renewable energy supplied at the beginning of the chain, resulting the hydrogen transport by ship in higher energy consumption than transporting methanol.

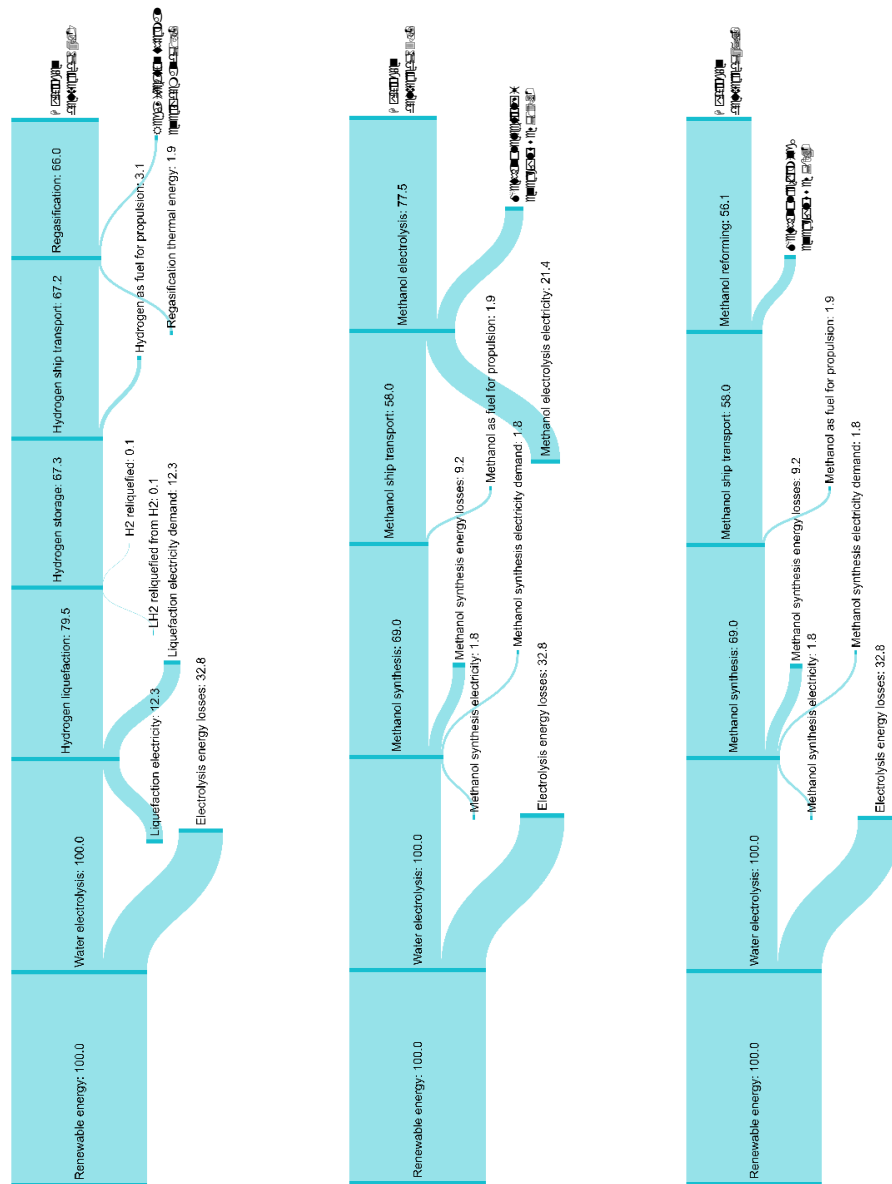


Figure 4. Process energy flow diagram for an annual production of 10 Mt of hydrogen. From left to right: hydrogen power link, methanol transport and electrolysis alternative, methanol transport and reforming alternative. 1,787 PJ/y is set at an index value of 100.

5. Conclusions

This work presents an energy study comparing three alternatives for transporting renewable energy under the form of fuels, delivering hydrogen at destination. The first alternative is based on the use of liquefied hydrogen as an energy vector. The second is based on the use of methanol as hydrogen vector, with a subsequent electrolysis process to obtain hydrogen at the destination. The third one also considers the methanol vector, but a methanol reforming process is used to obtain hydrogen. This work considers three mass flow rates of hydrogen produced: 100 kt/y, 1 Mt/y and 10 Mt/y, to make the comparison between the alternatives presented.

Comparison of the results obtained for the three power links show that the most interesting alternative in terms of energy is the transport of liquefied hydrogen. Transformation of H_2 in MeOH (methanol synthesis) and the subsequent reconversion of MeOH into H_2 (methanol electrolysis or reforming processes) implies more inefficiencies than liquefaction or regassification of H_2 , so the alternative based on the transport of liquefied hydrogen is the one that allows receiving a greater mass flow rate of hydrogen at destination with the lowest energy losses.

Comparing the power links based on methanol as hydrogen vector, the alternative that provides the greatest mass flow rate of hydrogen at destination is the electrolysis of methanol, due to the electricity consumed at destination. However, despite obtaining a smaller mass flow rate of hydrogen, the methanol reforming process is more independent of the electrical grid at destination.

Considering the electrical energy necessary at destination for the methanol electrolysis facility, it can be seen that research in this process could facilitate its development and produce a decrease in the energy consumption. This would modify the results shown, and the electricity demand and energy losses of this alternative could be closer or better to the ones obtained through the alternative of transporting liquid hydrogen.

6. References

- [1] S. S. Pethaiah, K. K. Sadasivuni, A. Jayakumar, D. Ponnamma, C. S. Tiwary and G. Sasikumar (2020). Methanol Electrolysis for Hydrogen Production Using Polymer Electrolyte Membrane: A Mini-Review. *Energies*, 13 (22), 5879.
- [2] R. D'Amore-Domenech, T. J. Leo and B. G. Pollet (2021). Bulk power transmission at sea: Life cycle cost comparison of electricity and hydrogen as energy vectors. *Applied Energy*, 288, 116625.
- [3] A. Basile and F. Dalena (2018). Methanol: Science and Engineering [online]. *Elsevier*.
- [4] A. Godula-Jopek, D. Stolten (2015). Hydrogen Production: by Electrolysis. *Wiley-VCH*.
- [5] U. Cardella, L. Decker, J. Sundberg and H. Klein (2017). Process optimization for large-scale hydrogen liquefaction. *International Journal of Hydrogen Energy*, 42(17), 12339–12354.
- [6] Kawasaki Heavy Industries, Ltd (2019). World's First Liquefied Hydrogen Carrier SUISEI FRONTIER Launches Building an International Hydrogen Energy Supply Chain Aimed at Carbon-free Society. [Accessed 18 January 2022]. Available from: https://global.kawasaki.com/en/corp/newsroom/news/detail/?f=20191211_3487&wovn=es
- [7] R. P. Sinha and W. Mohd Norsani (2012). Investigation of propulsion system for large LNG ships. *IOP Conference Series: Materials Science and Engineering*, 36(1), 012004.
- [8] R. Faizal and M. Holmlund-Sund (2015). Wärtsilä's energy efficient propulsion system selected by Indonesian owner for world's first ever CNG carrier. *Wärtsilä Corporation*. [Accessed 18 January 2022]. Available from: <https://www.wartsila.com/media/news/05-02-2015-wartsila's-energy-efficient-propulsion-system-selected-by-indonesian-owner-for-world's-first-ever-cng-carrier>
- [9] J. Nyári, M. Magdeldin, M. Larmi, M. Järvinen and A. Santasalo-Aarnio (2020). Techno-economic barriers of an industrial-scale methanol CCU-plant. *Journal of CO2 Utilization*, 39, 101166.
- [10] C. Lamy (2020). Electrocatalytic oxidation of low weight oxygenated organic compounds: A review on their use as a chemical source to produce either electricity in a Direct Oxidation Fuel Cell or clean hydrogen in an electrolysis cell. *Journal of Electroanalytical Chemistry*, 875, 114426.
- [11] M. Byun, B. Lee, H. Lee, S. Jung, H. Ji, and H. Lim (2020). Techno-economic and environmental assessment of methanol steam reforming for H_2 production at various scales. *International Journal of Hydrogen Energy*, 45 (46), 24146–24158.